Morphological characteristics of β-irradiated lead oxide nano-sized particles

O. Aldaghri [a], E. Y. Salih [b], A. Ramizy [c*], M. F. M. Sabri [d], N. Madkhali [a], T. Alinad [a], K. H. Ibnaouf [a], M. H. Eisa [a]

[a] *Department of Physics, College of Sciences, Imam Mohammad Ibn Saud Islamic University (IMSIU), Riyadh* 13318, *Saudi Arabia*

[b] *Department of Medical Physics, College of Medical Sciences Technologies, The University of Mashreq, 10021, Baghdad, Iraq*

[c] *Physics Department, College of Science, University of Anbar, Anbar, Iraq*

[d]*Nano Micro Engineering Laboratory, Faculty of Engineering, University of Malaya, 50603, Kuala Lumpur, Malaysia*

This work examined the beta irradiation and characterization of lead oxide nanoparticles samples that were prepared via pulsed laser deposition. The lead oxide nanoparticles samples were irradiated by beta-ray. Strontium 90 radioisotope was used as beta irradiation for different time periods (Days 1, 3, 4, and 5). The morphologies of lead oxide nanoparticles films were characterized with and without beta irradiation through the use of scanning electron microscope (SEM) and atomic force microscopy (AFM). According to the findings, beta radiation impacted lead oxide nanoparticles samples' morphological properties. The details of experimental setups, sample preparation procedures, and data analysis, are explicated.

(Received September 15, 2021; Accepted January 12, 2022)

Keywords: Lead oxide nanoparticles, Beta radiation, Band-gap, AFM, SEM

1. Introduction

Nanoparticles (NPs) denote a broad array of materials [1]. Of these, lead oxide (PbO) has been most intensively examined [2]. The PbO-NPs possess several outstanding properties, including the high surface area and nanoscale size [3-6]. Various oxide materials like PbO are usually wide-bandgap compounds. For these characteristics, PbO-NPs denote attractive materials that are regarded as feasible for various applications [6-9]. The significance of these materials is found in many applications and devices [9-15]. PbO-NPs can also be utilized in batteries [15], as a photocatalyst in the degradation of methyl blue dye [16], and in biomedical applications [17]. PbO-NPs' characterization and synthesis signify plenty of potential in various scientific fields [18-27]. In this context, several synthesis methods, such as the sol-gel [14], sonochemical [21], spray pyrolysis [22], chemical deposition [23], electrochemical method [24], microwave-assisted method [25], calcination [26], as well as PLD or pulsed laser deposition [27] have been used for PbO-NPs. In this context, PLD has also proven to be a versatile technique, particularly in producing high-quality complex nanostructured materials, such as PbO-NPs films.

The lead oxide nanostructures' morphology properties were investigated by using SEM and AFM characterization techniques. Today, it is becoming increasingly important to safeguard effective radiation shielding as space/nuclear/pharmaceutical industries require stronger, lighter, and radiation-resistant materials such as PbO-NPs. In this context, many works have been undertaken to examine radiation's impact on nanoparticle materials. However, it is also necessary to carry out studies to determine radiation effects on semiconductor devices for radiation tolerance. Therefore, many fundamental issues need to be investigated when irradiation is applied to the production or utilization of nanomaterials. However, several papers are dedicated to investigating radiation hardness on materials for X-rays, UV light, electron beams (beta irradiation) [28],

* Corresponding author: asmat_hadithi@uoanbar.edu.iq

gamma-radiation, ions, and neutrons [29-32]. More specifically, the interaction between light beams and electrons in materials is the cornerstone for several practical effects.

Furthermore, there is limited data available on the effect of beta irradiated on nanomaterials in the extant literature [31]. In this work, strontium 90 (Sr-90) radioisotope (with 2.86 m Ci activity)) gets utilized as a source of beta-ray (β- ray). Sr-90 is known as a bone seeker exhibiting biomedical behavior that bears similarity with calcium [32]. Thus, Sr-90 is extensively used as a radioactive source in medicine, especially as radiotherapy to treat some kinds of cancer [32]. Against this backdrop, this work aims to investigate beta radiation's impact on PbO-NPs via the use of Sr-90.

2. Experimental details

2.1. PbO Nanoparticles Preparation

This work utilized materials/reagents obtained from Iraq-based Sigma-Aldrich. Before being used, all samples were distilled two times with distilled water. To synthesize PbO powder, PLD method was employed; its purity level was found to be extremely at 99.99% with these precursors: lead nitrate and lead acetate. This process entails several mechanisms. The resulting mechanism, the lead acetate NaOH solution, was reacted with the lead nitrate Pb $(NO_3)_2$ solution for 15 min [28]. The sample consisting of yellowish-green precipitate was filtered before being washed using acetone and surplus distilled water. Thereafter, this sample was placed in an oven for drying for 24 hours. The dried sample was prepared under the force of 5 tons at room temperature for 3-5 min. Furthermore, the sample of 1.2 cm in diameter and 0.2 cm in thickness was obtained by pumping down the pressure to 10^{-3} Torr.

Subsequently, the dried sample was stored in a sealed container. Before depositing the substrates, detergent, glass substrates were cleaned using acetone, ethanol, deionized water, and chromic acid. The dried clean glass slide was then inserted in a beaker full of distilled water for 10 minutes before being rinsed. A soft tissue paper was used to wipe the glass substrates after they were blow-dried.

Via the PLD method, this sample was inserted into the glass substrate by utilizing the Nd-YAG laser. In the TEM00 mode, this Nd-YAG laser provides harmonic outputs of 1064 nm and532 nm. The focused q-switched laser system deposited the sample with a laser pulse duration of 10ns, a repetition frequency of 6Hz. The pulse number was at 500 with laser energy of 100 mJ, respectively. The laser beam's direction was toward the target surface using MgF2 lens with a focal length of 10cm situated outside the chamber of deposition; a distance of 2 cm was fixed between the substrate as well as the target. To prevent local damage, the target was then rotated.

Before being deposited, the PLD chamber was evacuated to a base pressure of ~10-3 Torr to attain an optimum condition. The focused laser beams were introduced from a high vacuum chamber at an incidence angle of 45º relative to the target surface. The target's rotation during the process of deposition was intended to avert local heating and drilling. When the films were grown using the PLD method, the deposition rate was calibrated to regulate the thickness. The set-up of the PLD method experiment details is given elsewhere [27]. All samples were labeled as a control (S0), the one-day irradiation (S1), the three- day irradiation (S3), the four-day irradiation (S4), and the five-day irradiation (S5), respectively. Total ionization dose experiments were conducted in collaboration with the Research Laboratory, Physics Department, College of Science, and Baghdad University, Iraq. The films were exposed to beta rays via a ^{90}Sr source. The geometry of the ^{90}Sr beta source surrounds the sample, causing isotropic exposure and obliterating the effects of directionality. Spectroscopies of SEM and AFM were used to investigate the morphological properties of the samples.

3. Results and discussion

3.1. AFM Results

The surfaces morphology of PbO films was performed in tapping mode by the AFM method. AFM was performed to examine the surface morphology and to measure roughness values for S0, S1, S3, S4, and S5. The manufacturer's software available with the microscope was utilized for measuring the variation of rms roughness as well as the hills' dimensions (average height and diameter) with beta-ray irradiation provided in Table 1. The root means square (rms) roughness of the film is calculated to be S0 (5.90 nm), S1 (12.50 nm), S3 (2.97 nm), S5 (1.38 nm), and S5 (2.50 nm). The roughness average is S0 (5.00 nm), S1 (10.50 nm), S3 (2.55 nm), S5 (1.16 nm), and S5 (2.15 nm). The peak is

S0 (22.80 nm), S1 (9.98 nm), S3 (5.48 nm), S5 (11.30 nm), and S5 (42.90 nm). These results reveal that the beta-ray irradiated surface of S1, S3, S4, and S5 was rougher compared to the S0 surface. Beta irradiation of PbO caused a slight change of the parameters as shown in Table 1.

The interaction of the beta-ray with the PbO film seemingly resulted in the irradiated film being altered. An important parameter that must be considered is surface morphology roughness. Hence, Table 1 determines average roughness (Ra). The Ra for irradiated sample surface reduces from 10.50nm to 2.15nm with beta-ray irradiation in comparison to S0 with the exception of S1. The film's roughness surface had risen after a slight rise in values on the irradiated surface by beta radiation at one day (S1). In addition, the surface's rms roughness reduced from 5.90 nm to 1.38 nm except for S1, as shown in Table 1.

Table 1 clearly shows that the surface skewness for S4 is far more positive. However, since the irradiation occurs within the sample, the value of the surface skewness becomes positive in S1, negative in S3, positive in S4 and negative in S5. For sample S0, the value of kurtosis is more than that of samples S1, S4, and S5. A significant observation of these high kurtosis values is shown in sample S3.

Table 1. AFM data from the samples after beta-ray irradiation.

Parameters	Sample				
	Before Irradiation	After Irradiation			
	S0	S1	S3	S4	S5
Roughness average (Ra) (nm)	5.00	10.50	2.55	1.16	2.15
RMS roughness (Rq) (nm)	5.90	12.50	2.97	1.38	2.50
SCK [Surface Skewness]	-0.23	0.03	-0.27	0.013	-0.18
SKU [Surface kurtosis]	2.06	1.87	2.09	1.93	1.86
Peak – Peak (nm)	22.8	8.98	5.48	11.30	42.90
Surface Area Ratio	10.90	2.80	0.91	2.89	28.80
Surface Bearing Index (nm)	3.57	3.39	1.65	2.60	7.45
Core Roughness Depth (nm)	17.70	7.64	3.84	9.62	36.00
Reduced Valley Depth (nm)	4.59	0.33	1.10	0.64	7.08

The results of samples in two three-dimensional topographic scans and granularity distributions can be seen in Figures 1 to 5. AFM images have informed the surface of the irradiated PbO thin film changed slightly. There is a slight agglomeration tendency before the beta irradiation process in the film. The unirradiated sample of PbO in Figure 6a illustrated globular formations, whereas the irradiated sample of Figures 6b to 6e was smaller and spherically shaped formations. However, the film's surface had finer surfaces (in Figure 6b) after the irradiation process. Figures 1 to 5 show the large sizes are formed and the surfaces are changed in the sample S1 to S5 compared to S0. The peaks height of the samples is also changed.

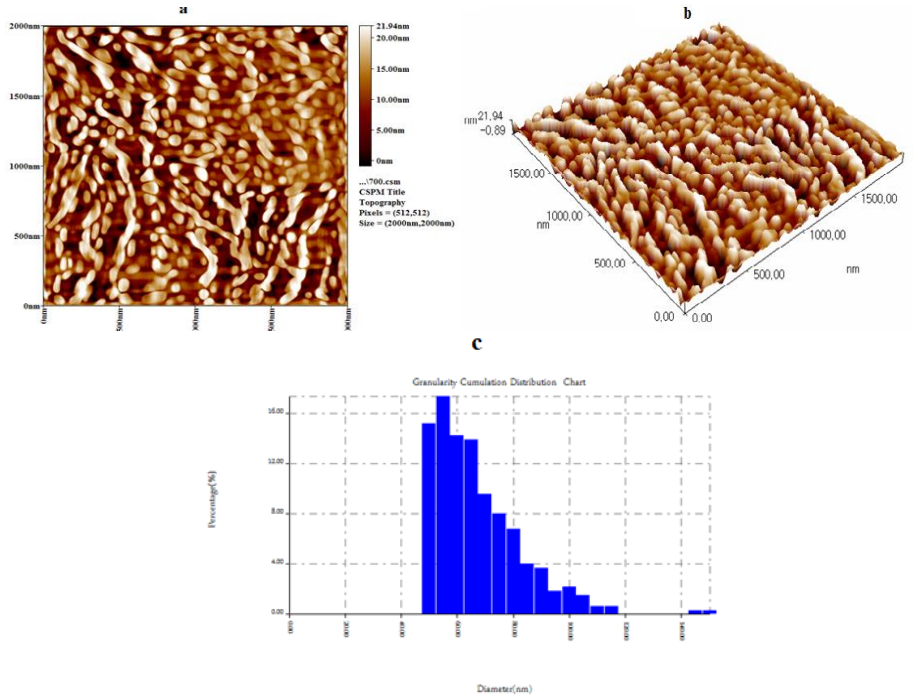

Fig. 1. AFM surface morphology of unirradiated PbO film a) 2-D, b) 3-D, and c) granularity distribution.

The biggest difference can be seen in the 2-D and the 3-D images of the S5. As evidenced by the results, the reduced valleys are predominated in the surface morphology and it becomes more planer. The unirradiated samples had an irregular shape, while their irradiated counterparts had regular (spherical) shapes and smaller-sized formations. Thus, the AFM images of the irradiated PbO thin film revealed that the grains are more spherical and homogeneously distributed over the entire surface when compared to the unirradiated PbO film. The AFM topography of irradiated films showed that the texture of the film surface has a waviness.

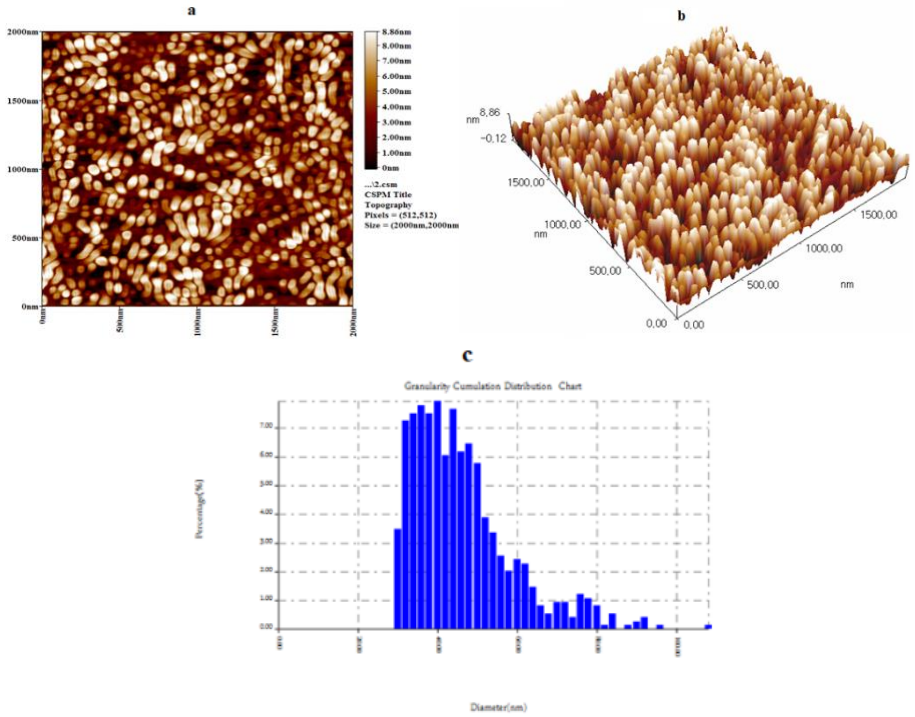

Fig. 2. PbO film's AFM surface morphology irradiated for one day a) 2-D, b) 3-D, and c) granularity distribution.

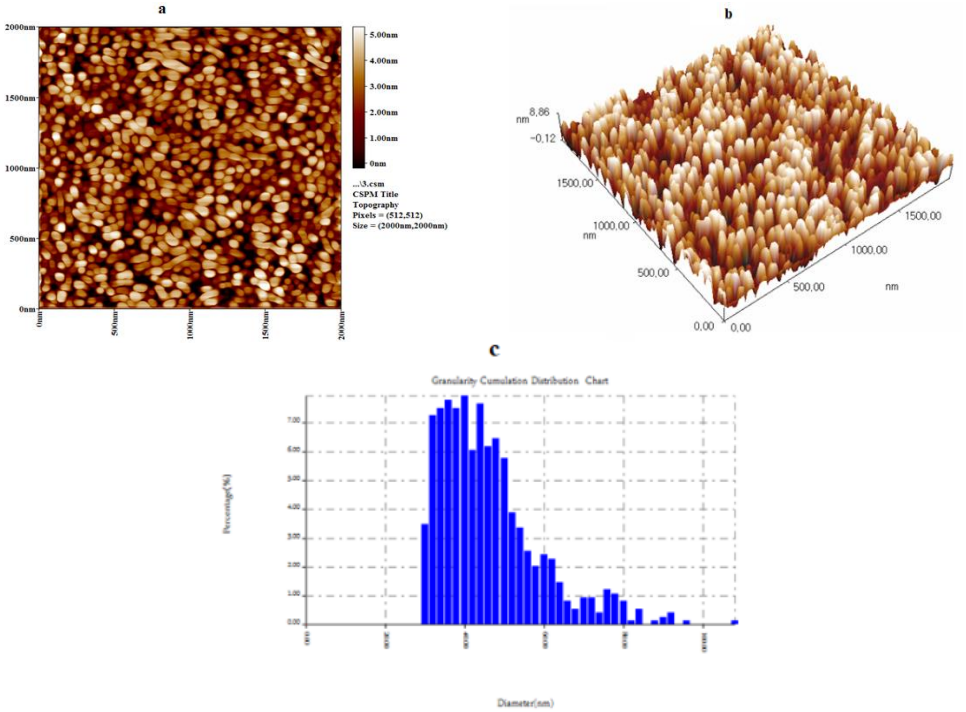

Fig. 3. AFM surface morphology of PbO film irradiated for three days a) 2-D, b) 3-D, and c) granularity distribution.

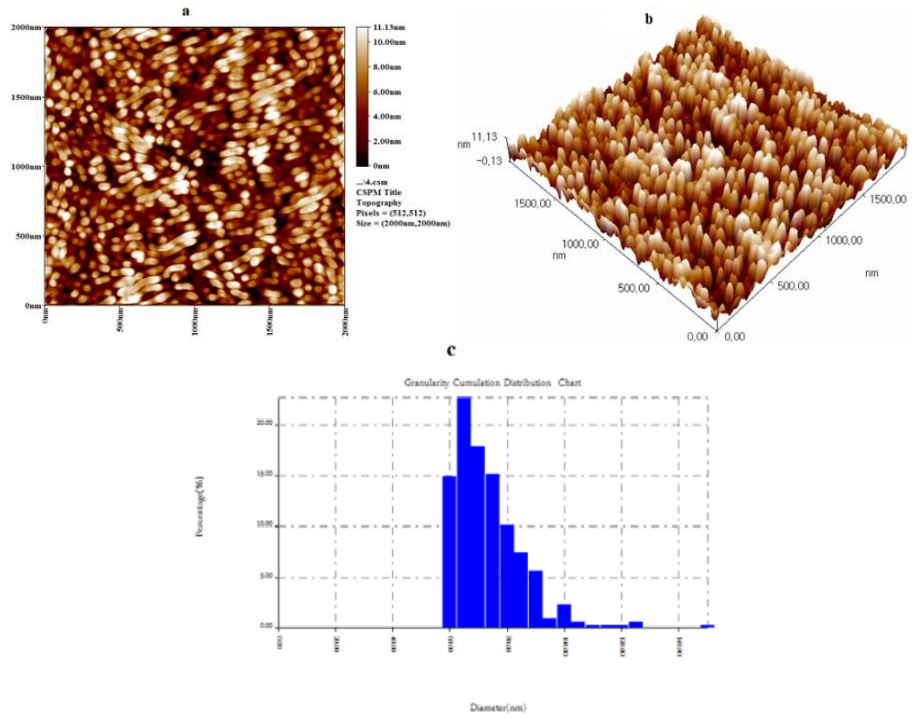

Fig. 4. PbO films' AFM surface morphology irradiated for four days a) 2-D, b) 3-D, and c) granularity distribution.

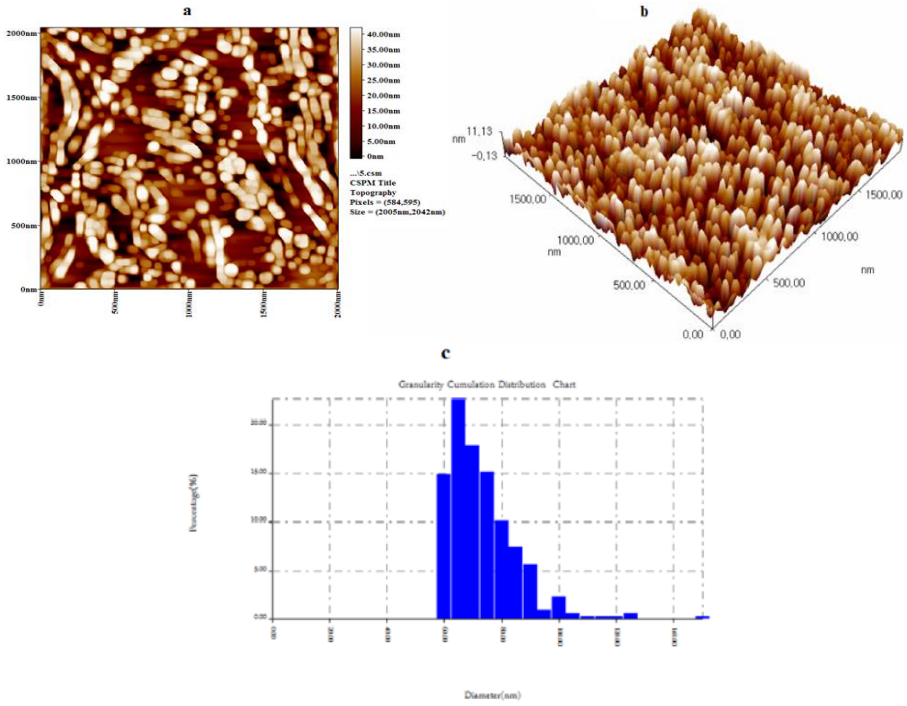

Fig. 5. PbO films' AFM surface morphology irradiated for five days a) 2-D, b) 3-D, and c) granularity distribution.

3.2. SEM Results

This study utilized SEM was used to evaluate the morphology of both unirradiated and irradiated PbO films. The unirradiated sample and the irradiated samples are shown in Figure 6. As shown by the SEM images, their materials were changed after beta irradiation. The grain size (D) of PbO nanoparticles was determined by SEM before and after β-ray irradiation. The grain size was found to get smaller in size after beta irradiation. From the SEM image of PbO samples, it becomes evident that the samples' surface and particles have a significant difference after irradiation. The nanoparticles have an almost spherical structure that a difference exists between the unirradiated and irradiated samples. The particles cling together to form a cluster in the unirradiated samples, but the irradiated samples saw a change in the nanoparticles' distribution. The SEM image shows that the particles' topology was out of place. Interaction of beta radiation was found to result in a minor alteration in terms of the parameters relating to PbO-NPs samples' surface.

The unirradiated samples' agglomeration is probably attributed to the challenge in getting them separated into single molecules of smaller size. These results are in congruence with the findings of extant literature [15]. The SEM images also revealed a wide distribution concerning particle size. SEM morphology of the obtained PbO powders for one day is larger and less uniform than those irradiated for five days. As per our studies, it is possible to control the size and shape parameters of the nanoparticle samples by using beta ray irradiation. A comparison of the samples' SEM images before and after the beta ray irradiation process showed that the samples' morphology is irregular-shaped before irradiation, as shown in Fig. 6a. During the period of high irradiation (5 days), the samples' SEM images illustrate the most uniform and smallest particles, as depicted in Fig. 6e.

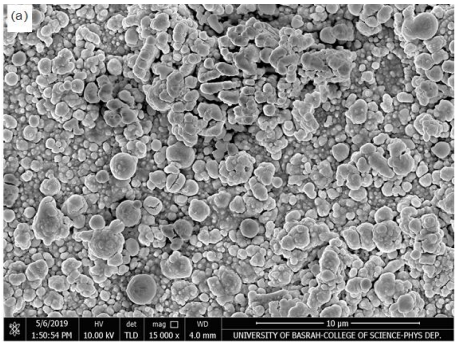

Fig. 6. a SEM micrographs for PbO films before irradiation.

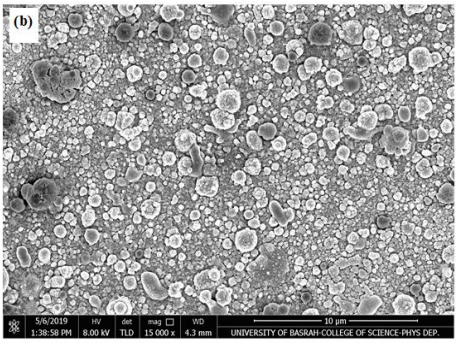

Fig. 6. b SEM micrographs of PbO films after irradiation for one day.

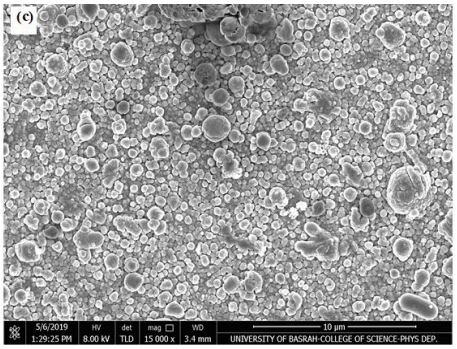

Fig. 6. c SEM micrographs of PbO films after irradiation for three days.

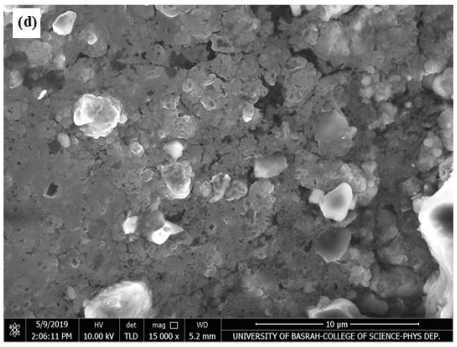

Fig. 6. d SEM micrographs of PbO films after irradiation for four days.

4. Conclusion

It can be included that the impact of beta-ray irradiation on PbO film leads to alterations in surface morphology up to a few nanometers. The PbO sample's roughness increases after a fluence increase of the irradiation caused by time duration. Unfortunately, there is a paucity of data for the AFM studies in lead oxides. As per the AFM studies, it is possible to control the size and the shape parameters of the nanoparticle samples by using beta ray irradiation. The irradiated films' AFM topography showed that the texture of the film surface has waviness. The analyses of the samples' SEM revealed that the days of beta ray irradiation impact the nanostructure materials' characteristics. After five days of irradiation, SEM images depict that the smallest samples had the most uniform particles, which indicated that the five-day irradiation time is optimal. The unexpected behavior of PbO-NPs films irradiated with beta-rays, as investigated study, could be ascribed to the irradiation's time interval. In the un-irradiated sample, the particles cling together to form a cluster, but the distribution of the nanoparticles was changed in irradiated samples. A significant difference occurs at irradiation of sample PbO-5, where the film surface exhibits a higher roughness and clear grains were observed. Beta irradiation caused alterations in the morphological properties of the film.

Acknowledgements

The authors express their gratitude to the Deanship of Scientific Research at Imam Mohammad Ibn Saud Islamic University which funded their work via Research Group no. RG-21-09-44.

References

[1] E. Y. Salih, M. F. M. Sabri, M. H. Eisa, K. Silaiman, A. Ramizy, M. Z. Hussein, S. M. Said, Materials Science in Semiconductor Processing **121**, 105370 (2021).
[2] T. J. Wilkinson, D. L. Perry, E. Spiller, P. Berdah, S. E. Derenzo M. J. Weber, Proceed. Mater. Res. Soc. **704**, 117 (2002).
[3] M. K. Mahmoudabad, M. M. Motlagh, IJPS **6**(24), 5720 (2011).
[4] T. Mahalingam, S. Velumani, M. Raja, S. Thanikaikarasan, J. P. Chu, S. F. Wang, Y. D. Kim, Materials Characterization **58**, 817 (2007).
[5] S. Sriram, R. Chandiramouli, P. Gopinath, Asian Journal of Applied Sciences **7**(8), 774 (2014).
[6] H. M. Arafa, W JPS **2**(12), 1947 (2014).
[7] R. Yousefi, A. K. Zak, F. J. Sheini, W. J. Basirun, CI **40**, 11699 (2014).
[8] M. M. Kashani-Motlagh, M. Karami Mahmoudabad, Journal of Sol-Gel Science and Technology **59**(1), 06 (2011).
[9] M. Alagar, T. Theivasanthi, A. Kubera Raja, Journal of Applied Sciences **12**(4), 98 (2012).
[10] K.-C. Chen, C.-W. Wang, Y.-I. Lee, H.-G. Liu, Colloids and Surfaces A: Physicochemical and Engineering Aspects **373**(1), 124 (2011).
[11] L. Li, X. Zhu, D. Yang, L. Gao, J. Liu, R. Vasant Kumar et al., Journal of Hazardous Materials **203-204**, 74 (2012).
[12] N. Gandhi, D. Sirisha, S. Asthana, International Journal of Engineering Sciences and Research Technology **7**(1), 623 (2018).
[13] M. A. Shah, International Journal of Biomedical Nanoscience and Nanotechnology **1**(1), 3 (2010).
[14] H. Karami, M. Ghamooshi-Ramandi, International Journal of Electrochemical Science **8**, 7553 (2013).
[15] A. V. Borhade, D. R. Tope, B. K. Uphade, Journal of Chemistry **9**(2), 705 (2012).
[16] H. Karami, M. A Karimi, S. Haghdar, A Sadeghi, R. M. Ghasemi, S. M. Khani, Mater. Chem. Phys. 108(2-3), 337 (2008).

[17] M. A. Shah, International Journal of Biomedical Nanoscience and Nanotechnology **1**(1), 3 (2010).
[18] Jaison Jeevanandam, Ahmed Barhoum, Yen S. Chan, Alain Dufresne, Michael K. Danquah, Brillstein J. Nanotechnol. **9**, 1050 (2018).
[19] T. Theivasanthi, M. K. Alagar, physics. chem., 1 (2012).
[20] M. K. Mahmoudabad, M. M. Kashani-Motlagh, International Journal of Physical Sciences **6**(24), 5720 (2011).
[21] A. Morsali, L. Hashemi, Journal of Nanostructures **1**(2), 89 (2011).
[22] M. Suganya, A. R. Balu, K. Usharani, M. Sci. **32**(3), 448 (2014).
[23] N. Mythili, K. T. Arulmozhi, IJS. & Eng. R. **5**(1), 412 (2014).
[24] H. Karami, M. Alipour, Journal of Power Sources **191**(2), 653 (2009).
[25] V. S. R. Raju, S. Murthy, F. Gao, Q. Lu, S. Komarneni, Journal of materials science **41**(5), 1475 (2006).
[26] L. Li, X. Zhu, D. Yang, L. Gao, J. Liu, R. V. Kumar, J. Yang, Journal of hazardous materials **203**, 274 (2012).
[27] Hassan Karami, Mahboobeh Alipour, Int. J. Electrochem. Sci. **4**, 1511 (2009).
[28] M. H. Eisa, Materials Science in Semiconductor Processing, Volume **110**, 104966 (2020).
[29] R. S. Benson, Nucl. Instrum. Methods Phys Res Sect B: Beam Interact Mater At. **191**, 752 (2002).
[30] R. A. Andrievski, Phys. Met. Metallogr. **110**(3), 229 (2010).
[31] R. A. Andrievski, Rev. Adv. Mater. Sci. **29**, 54 (2011).
[32] C. Wang, M. H. Eisa, W. Jin, H. Shen, Y. Mi, J. Gao, Y. Zhou, H. Yao, Y. Zhao, Nuclear Instruments and Methods in Physics Research B **266**, 1619 (2008).